

# Wavelength dependent laser-induced etching of Cr–O doped GaAs: Morphology studies by SEM and AFM

B JOSHI, S S ISLAM\*, H S MAVI<sup>†</sup>, VINITA KUMARI, T ISLAM<sup>††</sup>, A K SHUKLA<sup>†</sup> and HARSH<sup>#</sup>

Department of Applied Sciences and Humanities,<sup>††</sup>Department of Electrical Engineering,  
Faculty of Engineering and Technology, Jamia Millia Islamia (Central University),  
New Delhi 110 025, India

<sup>†</sup>Department of Physics, Indian Institute of Technology, New Delhi 110 016, India

<sup>#</sup>Solid State Physics Laboratory (DRDO), Lucknow Road, Delhi 110 054, India

MS received 16 May 2008

**Abstract.** The laser induced etching of semi-insulating GaAs  $\langle 100 \rangle$  is carried out to create porous structure under super- and sub-bandgap photon illumination ( $h\nu$ ). The etching mechanism is different for these separate illuminations where defect states play the key role in making distinction between these two processes. Separate models are proposed for both the cases to explain the etching efficiency. It is observed that under sub-bandgap photon illumination the etching process starts vigorously through the mediation of intermediate defect states. The defect states initiate the pits formation and subsequently pore propagation occurs due to asymmetric electric field in the pore. Formation of GaAs nanostructures is observed using scanning electron microscopy (SEM) and atomic force microscopy (AFM).

**Keywords.** Laser-induced etching; intermediate state; nanostructure; SEM; AFM.

## 1. Introduction

Laser-induced etching, an improved etching process, is very much needed in the fabrication of III–V integrated optic and microelectronic devices (Syvenkyy *et al* 2005; Veiko *et al* 2005; Yi and Parker 2006). Several studies of laser induced etching have shown the importance of its higher processing rate than the conventional etching techniques (Svorcik and Rtybka 1989; Cha *et al* 1997; Han *et al* 1998; Simkiene *et al* 2003). With this technique the etching is initiated nonthermally by light-generated electron-hole pairs, which diffuses to the surface and greatly enhances the oxidation-reduction reaction between the semiconductor and a dilute acid solution. The dissolution kinetics is very complex in III–V semiconductors; its sophisticated nature and much of its properties are not fully understood till date. In spite of several decades of intense research into the properties and applications of GaAs, the surface chemistry of this material has only recently began to be investigated in a systematic fashion.

The present study reports the laser-induced etching process in semi-insulating GaAs  $\langle 100 \rangle$  in HF solution under both super- and sub-bandgap photon illuminations ( $h\nu$ ). It is found that the bandgap photon illumination,

though an essential criterion in case of semiconductor etching, is not so crucial to determine the etching rate in semi-insulating GaAs; rather the impurity and defect states in as-grown GaAs plays the key role. The reaction rate analysis at the semiconductor–electrolyte interface shows that the reaction rate is much faster in case of sub-bandgap illumination. The interpretation is given with suitable demonstration of excess carrier processes. The surface morphology studies by SEM and AFM also show the formation of qualitatively superior nanostructure under sub-bandgap photon illumination.

## 2. Experimental

Two pieces of samples were prepared from Cr–O doped GaAs  $\langle 100 \rangle$  wafer with a resistivity of  $10^7$  ohm-cm in HF solution. Prior to etching the samples were degreased with acetone, propane and methanol. The Cr content in the sample was roughly 1 wt. ppm. Laser-induced etching was done on sample-A using an argon-ion CW laser ( $\lambda = 514.5$  nm) and on sample-B by Nd:YAG laser ( $\lambda \sim 1.06$   $\mu\text{m}$ ) for 45 min while laser power density was kept fixed at  $20 \text{ W/cm}^2$ . After etching, the samples were rinsed with ethanol and dried in air with filtered  $\text{N}_2$ . The surface analysis was done by using scanning electron microscopy (SEM, JEOL 6330) and atomic force microscopy (AFM, RN-2, Pacific Nanotechnology).

\*Author for correspondence (safiu\_el@rediffmail.com)

### 3. Results and discussion

#### 3.1 Surface morphology and laser-induced etching mechanism

SEM micrographs of the etched GaAs samples A and B are shown in figure 1. In figure 1(a) for sample-A (top image), pits like depression with irregular structures are

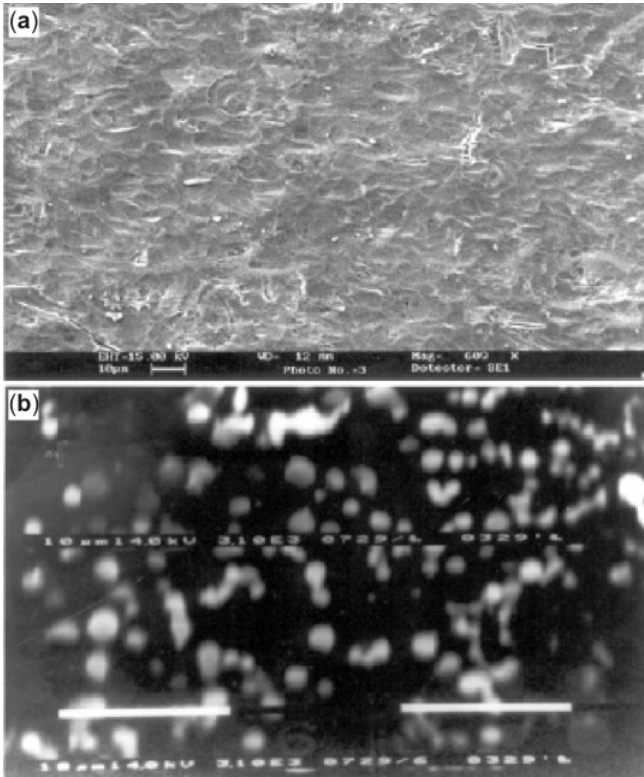


**Figure 1.** SEM micrographs of (a) sample-A and (b) sample B.

observed when the sample was irradiated with super-bandgap photon illumination of energy,  $h\nu >> E_g$ , where  $E_g$  is the bandgap of the semiconductor. The etching shows creation of shallow optical depth as visible from the micrograph. In figure 1(b) for sample-B (bottom image), the bright grain of material with range of size  $\sim 500$  nm to  $1\ \mu\text{m}$  on top of GaAs are observed. The average depth of etched layer is much more profound with  $3\ \mu\text{m}$  depth in sample B and it is 300 times higher than in sample A. The formation of GaAs micro-crystallites and its etched depth indicates the superiority in etching rate and efficiency in case of sub-bandgap photon illumination. A comparative study about the surface etching reaction rate at identical conditions except the photon energy used for illumination is shown in figure 2. It is observed that the reaction rate in case of sub-bandgap photon illumination is much faster than its counterpart. These results throw some new aspects vis-à-vis the conventional laser-induced etching in extrinsic type GaAs reported by other researchers (Yamamoto and Yano 1975; Cha *et al* 1997). The interpretation of the microscopic results is done in this report with the idea of photo-carrier generation and recombination via intermediate states associated with the defects of solids.

**3.1a Standard principle of laser-induced etching:** Reports on photoetching on semi-insulating GaAs is scarce in the literature. Few works have been reported so far on semi-insulating GaAs wafer (Simkiene *et al* 2003; Mavi *et al* 2004). Normal photoetching work on extrinsic GaAs with photon illumination energy,  $h\nu \geq E_g$  (bandgap), is proposed by several authors (Svorick *et al* 1997; Han *et al* 1998). Etching initiation for  $h\nu \leq E_g$  in semi-insulating GaAs is not in conformity with the earlier published reports. The interpretation is given with conceptual modification of the standard etching process of extrinsic semi-

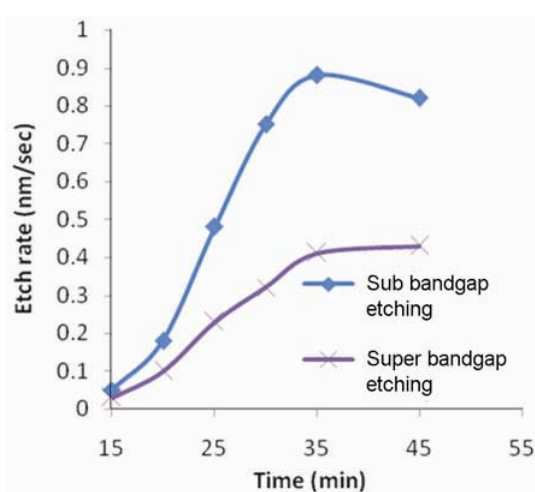


**Figure 2.** The etching rate as a function of etching duration for sample A.

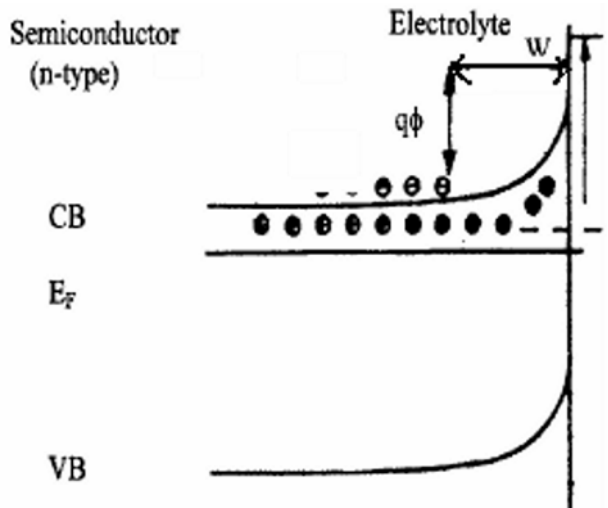


**Figure 3.** Schematic illustration of the band model for *n*-type semiconductor/electrolyte junction under photon illumination.

conductor having impurity as well as inherent defect states in the as grown samples.

In laser-induced chemical etching, the semiconductor is immersed in a conductive electrolyte and the sample surface is irradiated with photon beam of energy  $\geq$  bandgap ( $E_g$ ) of the semiconductor. Figure 3 shows the case of *n*-type semiconductor in contact with an electrolyte. The charge density in the semiconductor space-charge layer is  $qN_D$ , where  $N_D$  is the donor concentration. Therefore,

$$\nabla E = (qN_D/\epsilon), \quad (1)$$

where  $\epsilon$  is the dielectric permittivity of the semiconductor,  $E$  the electric field, and  $q$  the magnitude of the electronic charge. The width of the space-charge region,  $W$ , is related to the potential drop,  $\phi$ ,

$$W = \sqrt{\frac{2\epsilon\phi}{qN_D}}. \quad (2)$$

On illumination, the  $e-h$  pairs created within the space-charge region are transported by migration under the influence of the electric field, and diffusion due to the gradient in the carrier concentration. The hole concentration,  $p$ , is determined from the transport relation for the hole current density,  $J_p$ ,

$$J_p = q\mu_p p E - qD_p \nabla p, \quad (3)$$

where  $D_p$  is the hole diffusion constant and  $\mu_p$  the hole mobility. Photogenerated holes (minority carriers in *n*-type semiconductors) which reach the semiconductor-electrolyte interface can react with solution species. Thus, the energy gap and electric field act as a kinetic barrier for electrons (majority carriers in *n*-type semiconductors) to reach the semiconductor-solution interface. The system is analogous to a semiconductor-metal photodiode, except that ionic conduction replaces the electronic conduction in the metal.

### 3.1b Laser-induced etching of Cr–O doped GaAs for super- and sub-bandgap photon illumination:

The sample

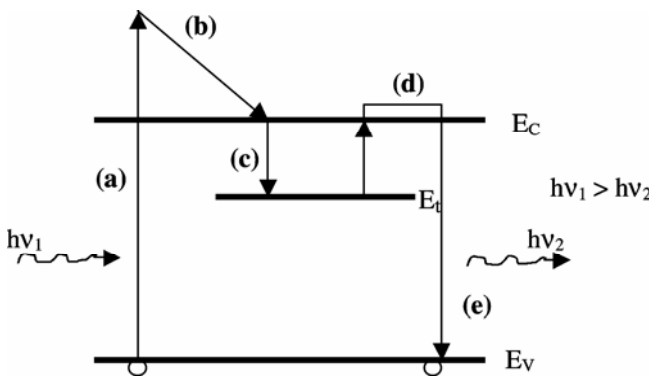


**Figure 4.** Direct excitation and recombination mechanisms in semiconductor with a trapping level for electrons.

under study is GaAs doped with two species, Cr and O. It is semi-insulating, i.e. highly resistive. Therefore, (1) and (2) are to be replaced by the term  $|N_D - N_A|$ , where  $N_A$  is the acceptor concentration. Under photon illumination of energy 2.41 eV, i.e.  $h\nu \gg E_g$ , it is expected that  $e-h$  pair generation rate will be quite strong for band-to-band transition and etching phenomena should occur strongly. The SEM results show something contrary to the expectations. The fact was explained by a simple demonstration shown in figure 4. GaAs is well known to have defect states in the forbidden gap due to dislocation and surface defects ( $E_t$ ). The as grown etch pits density of the sample is  $\sim 7000/cm^2$ . The generation and recombination of  $e-h$  pairs under illumination with photon of energy, 2.41 eV, are described in four processes. In process (a) one electron is lifted from valence band to deep inside the conduction band; one  $e-h$  pair is generated. In process (b), the excited electron gives up its energy to the lattice by scattering until it percolates to the bottom of the conduction band. In process (c) the electron is trapped by the impurity level,  $E_t$  and remains trapped until it can be thermally re-excited to the conduction band (shown in

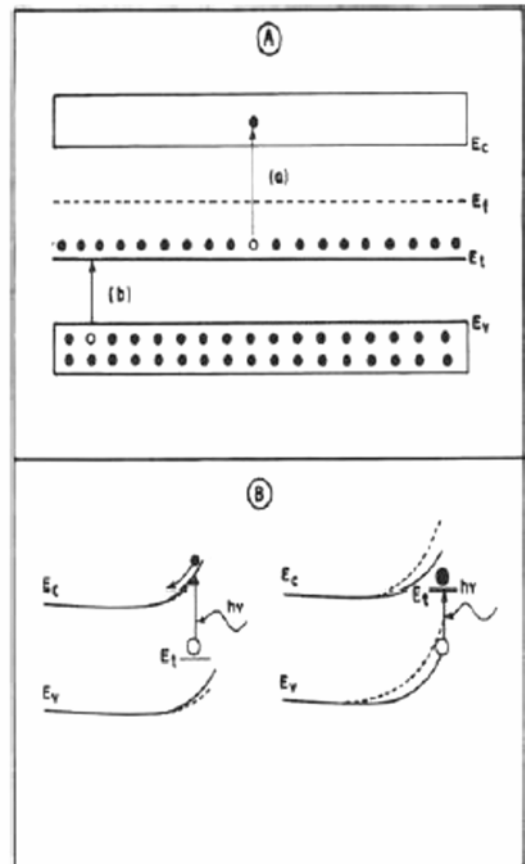


**Figure 5.** Schematic band diagrams of the surface space charge region at semiconductor/electrolyte interface under sub-bandgap illumination with excitation of trapped (A) electrons and (B) holes.  $E_t$  represents one defect state below  $E_f$  at equilibrium.

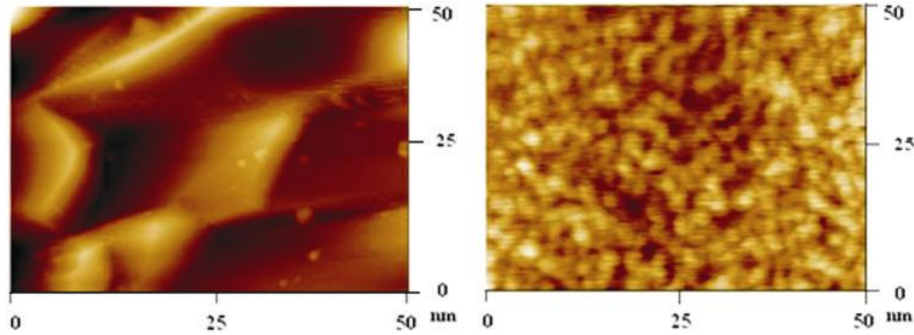


**Figure 6.** AFM micrograph of samples A and B etched at laser power,  $30 \text{ W/cm}^2$ , for etching time, 45 min.

process (d)). In process (e) finally direct recombination occurs as the electron falls to an empty state in the valence band, giving off a photon of energy  $h\nu$ . The delay time in the recombination process is due to the increase of life time of the electron in the conduction band and it can be relatively long due to two important factors: (i) high density of defect states, and (ii) the low probability of thermal re-excitation. Recombination process is shown here to calculate the generation rate and at steady state, recombination and generation rates balance each other. Therefore, normal  $e-h$  pair generation will be very slow in case of band-to-band transition and it is strongly hampered due to the presence of defect states which do not act as stepping stones to facilitate the generation process. This may be one reason for less hole supply to the semiconductor-electrolyte interface. It results in low oxidation-and dissolution rate and subsequently, the slow etching process. Experimentally it has been verified that negligible improvement in surface etching takes place even at high laser power; whereas, excellent porous structure is prepared for  $h\nu < E_g$  at low level laser power as reported by the present authors (Mavi *et al* 2004).

**3.1c Laser-induced etching of Cr-O doped GaAs for sub-bandgap photon illumination:** Laser-induced etching of semi-insulating GaAs for  $h\nu \ll E_g$  can be understood through this mechanism. Any impurity or lattice defect can serve as a generation/recombination centre if it is capable of receiving a carrier of one type and subsequently capturing the opposite type of carrier, thereby generating/annihilating the pair. One such example is demonstrated in figure 5.  $E_t$  represents one defect state below  $E_F$  at equilibrium and therefore, is substantially filled with electrons. The defect state will be filled or partially filled depending upon the relative positions with respect to the extrinsic Fermi level position. Excess  $e-h$  pair generation occurs in two steps: (a) hole capture and (b) electron capture. It is important to note that the first event is equivalent to an electron excited from  $E_t$  to the conduction band creating a hole in the defect state. In the second event, the hole is transferred to the valence band

by an electron excitation from the valence band to  $E_t$ . When both these events occurred, the defect state is back to its original state. The photo-generated holes drift to the interface and the electron is swept away from the interface due to the electric field in the interface. Then follows surface oxidation and dissolution to create pores. The photo-generated holes initiate an anodic reaction resulting in the formation of oxide which is soluble in electrolyte. The transport of these holes to the surface and their resultant spatial distribution, therefore, determines the morphology of the etched sample.

The subsequent phase is the pore formation and its propagation. Pits initiation is a prerequisite criteria for pore formation in the substrate. A pit will form at a point on the surface if the dissolution rate is enhanced at that point relative to elsewhere on the surface. The most important etch pit is the one associated with the point of emergence of a dislocation on the surface (Ross *et al* 1997). The localized etching process induces a pit which will have an increased electrical field strength at its tip and causes the pore size to propagate.

The formation of GaAs nanostructure is further confirmed by AFM studies on samples A and B after 45 min of etching duration keeping other parameters identical (Figure 6). The formation of nanocrystallite of size 3–5 nm in case of sample B and 12–15 nm in case of sample A. By combining SEM and AFM images of both the samples it may be interpreted that preparation of nanostructure in semi-insulating GaAs is more convenient under sub-bandgap photon illumination used in the etching process.

#### 4. Conclusions

Laser induced etching of Cr-O doped GaAs wafer is described by two models to explain the etching mechanism under super- and sub-bandgap photon illumination. Under super-bandgap illumination weak etching rate is observed which is in contradiction with the standard photo-induced etching principle. It is understood that the hole supply to the semiconductor-electrolyte interface is strong in case

of sub-bandgap photon illumination in comparison to its counterpart and the defect states play havoc with the rate of hole supply as well as etching rate. The formation of superior quality nanostructure is observed by SEM and AFM studies under sub-bandgap photon illumination where other etching parameters remained identical.

### Acknowledgement

One of the authors (SSJ) gratefully acknowledges the financial assistance by the Department of Science and Technology, Govt. of India, through its grant no. CMP-44/2004.

### References

- Cha C, Han B Y and Weaver J H 1997 *Surf. Sci.* **381** L636  
Han B Y, Cha C and Weaver J H 1998 *J. Vac. Sci. Technol.* **A16** 490
- Mavi H S, Islam S S, Rath S, Chauhan B S and Shukla A K 2004a *Mater. Chem. & Phys.* **86** 414  
Mavi H S, Shukla A K, Chauhan B S and Islam S S 2004b *Mater. Sci. & Engg.* **B107** 148  
Ross F M, Oskam G, Searson P C, Maculay J M and Liddle J A 1997 *Philos. Mag.* **A75** 525  
Simkiene A, Sabataityte T, Karpus V, Reza A, Babonas G J, Cechavicious B and Suchodolskis 2003 *Mater. Sci. & Engg.* **C23** 977  
Svorick V and Rtybka V 1989 *Chem. Phys. Lett.* **164** 549  
Svorick V, Rtybka V and Myslick V 1989 *Chem. Phys. Lett.* **157** 390  
Svorick V, Rtybka V and Myslick V 1997 *Chem. Phys. Lett.* **144** 548  
Syvenky Yu, Kotlyarchuk B, Zaginey A and Sahraoui B 2005 *Opt. Commun.* **256** 342  
Veiko V P, Kieu Q K, Nikonorov N V, Shur V Ya, Luches A and Rho S 2005 *Appl. Surf. Sci.* **248** 231  
Yamamoto A and Yano S 1975 *J. Electrochem. Soc.: Solid State Sci. & Technol.* **122** 260  
Yi E H and Parker M A 2006 *J. Electrochem. Soc.* **153** 496